# NO evaporative cooling in the $^2\Pi_{3/2}$ state

Lucie D. Augustovičová* and John L. Bohn
*JILA, NIST, and Department of Physics, University of Colorado, Boulder, Colorado 80309-0440, USA*

(Received 9 March 2018; published 8 June 2018)

The scattering at ultralow temperatures of fermionic $^{14}N^{16}O$ molecules in the metastable $^2\Pi_{3/2}$ is considered, under the influence of parallel electric and magnetic fields. It is found that a magnetic field of several thousand Gauss can enhance the ratio of elastic-to-inelastic collision rates. The magnetic field can therefore assist the electric field in increasing this ratio. Evaporative cooling of NO is feasible only in the presence of combined magnetic and electric fields and for temperatures above about 70 mK.

DOI: 10.1103/PhysRevA.97.062703

## I. INTRODUCTION

In a recent paper [1], we discussed the collision cross sections of ground-state nitric oxide (NO) molecules at low temperatures, below 1 K. This work was motivated by the possibility of evaporatively cooling this species, if it were to be produced in a sub-Kelvin sample by buffer-gas cooling, Stark deceleration, or other means [2–5]. In Ref. [1] it was found that elastic rate constants greatly exceed inelastic rate constants only at temperatures above about one hundred millikelvin. Evaporative cooling would therefore be limited to temperatures on this order, thus succumbing to the "millikelvin catastrophe" common in cold molecules [6–8].

In the $^2\Pi_{1/2}$ ground state considered in Ref. [1], the application of a very large electric field (of order tens of kV/cm) was found to suppress the inelastic rates, but this field is likely too large to usefully do so in the laboratory. The application of a magnetic field would do little to suppress collisions in this state, which has a negligible magnetic moment. By contrast, the metastable excited $^2\Pi_{3/2}$ state of NO does possess a magnetic moment and could in principle be influenced by magnetic, as well as electric, fields. Magnetic fields have been predicted to suppress inelastic scattering of $^2\Pi_{3/2}$ OH molecules [9–11], leading to ongoing efforts to achieve evaporative cooling in this radical [12].

In this paper we therefore extend the work of Ref. [1] to the metastable state of NO, studying the influence of combined (parallel) electric and magnetic fields on collision rates. While the addition of a magnetic field has some modest additional effect, the conclusion remains that evaporative cooling of NO below 100 mK is problematic.

## II. THEORY

### A. NO molecular structure in absence of external field

In this section we briefly describe the structure of the NO molecule. The NO ground-state structure is considered in Ref. [1], to which we refer readers for details. In the rigid-rotor approximation, the internal structure of the ground $^2\Pi$ electronic state, ground vibrational state includes the spin-orbit (SO) interaction, rotation (ROT), spin-rotation (SR) interaction, $\Lambda$-doubling structure, and nitrogen hyperfine interaction (HFS) in $^{14}N^{16}O$. The well-defined axial components $\Lambda$ and $\Sigma$ are combined to define $\Omega$, a good quantum number in the Hund's case-(a) representation. Components of $\Lambda$ doubling are $|\Omega| = 1/2$ and $|\Omega| = 3/2$, both doubly degenerate, of which $^2\Pi_{3/2}$ is the higher-lying state. Their separation is determined by a spin-orbit fitting parameter of 123.146 $cm^{-1}$ [13], far enough for neglecting the lower state in our cold-collision calculation. For these purposes the nearest rotational level $J = 5/2$ can be neglected because the $^{14}NO$ rotational constant is 1.696 $cm^{-1}$ [13].

The total angular momentum of the molecule $\vec{J}$ has definite projections on the space-fixed axis $M$ and on the molecule-fixed axis $\Omega$. The eigenvectors of $H_{SO} + H_{ROT} + H_{SR}$ for each $J$, $M$ are doubly degenerate in $\Omega$:

$$\left|^2\Pi^{\pm}_{3/2}\right\rangle = |\Lambda = \pm 1, S, \Sigma = \pm 1/2\rangle |\Omega = \pm 3/2, J, M\rangle. \quad (1)$$

In zero electric field, these states are combined into a parity doublet $+/-$. The parity basis is a linear combination of (1) that is labeled according to their total parity under the inversion operation $E^*$ for each rotational level,

$$\left|^2\Pi_{3/2}(+/-)\right\rangle = \frac{1}{\sqrt{2}}\left(\left|^2\Pi^{+}_{3/2}\right\rangle \pm (-1)^{J-S}\left|^2\Pi^{-}_{3/2}\right\rangle\right). \quad (2)$$

These functions can also be classified according to $p = e$ or $f$ symmetry, total parity exclusive of a $(-1)^{J-1/2}$ rotational factor. The $\Lambda$-doubling constant is $\Delta_\Lambda = 5 \times 10^{-5}$ K [14] which is about 350 times smaller than for the $^2\Pi_{1/2}$ state.

In addition, the $^{14}N$ nucleus has spin $I = 1$ (the spin of the $^{16}O$ nucleus is zero), we extend the basis function set to also include $\vec{I}$, coupled to $\vec{J}$ to form $\vec{F}$ in the laboratory frame, thus the $J = 3/2$ level of our interest splits into three hyperfine components $F = 1/2$, $F = 3/2$, and $F = 5/2$. This identifies the molecular basis set as $|\eta, |\Omega|, J, I, F, M_F; p\rangle$, where $M_F$ is the projection of $F$ onto the laboratory axis, and $\eta$ is a general index which represents all other quantum numbers. Within the $^2\Pi_{3/2}$, $J = 3/2$ manifold, we employ the shorthand notation $|F, M_F; p\rangle \equiv |\eta, |\Omega|, J, I, F, M_F; p\rangle$.

*Present address: Charles University, Faculty of Mathematics and Physics, Department of Chemical Physics and Optics, Ke Karlovu 3, CZ-12116 Prague 2, Czech Republic.

 

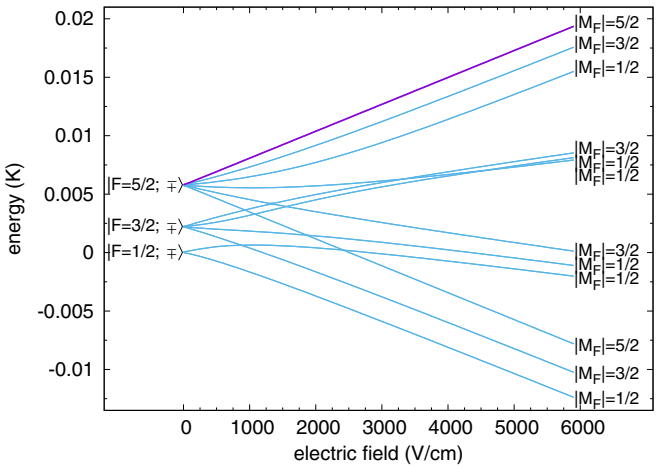


FIG. 1. Stark energies of the hyperfine $|F,M_F;e/f\rangle$ and $\Lambda$-doublet levels for $J=3/2$ of the $^2\Pi_{3/2}$ state of the NO molecule at zero magnetic field. Each line is doubly degenerate in $M_F$. The hyperfine state of our interest $|5/2,5/2;f\rangle$ is highlighted.

### B. Stark and Zeeman field interactions with NO

In the presence of a homogeneous electric field $\vec{\mathcal{E}}$ whose direction specifies the space-fixed $Z$ axis, the effective Hamiltonian is augmented by the Stark-effect term $H_S=-\vec{d}_s\cdot\vec{\mathcal{E}}$. The space-fixed component of the electric-dipole moment of the molecule $d_s^Z=T_0^1(\vec{d}_s)$ needs to be rotated to the molecule-fixed axis, to which the electric-dipole moment $\vec{d}_m$ is referred by using a Wigner $D$ matrix, $T_0^1(\vec{d}_s)=\sum_q D_{q0}^{(1)*}T_q^1(\vec{d}_m)$. The electric-field Hamiltonian becomes

$$H_S=-\mathcal{E}\sum_q D_{q0}^{(1)*}T_q^1(\vec{d}_m).$$

In the $|J,M,\Omega\rangle$ basis, matrix elements of $H_S$ are well known, and with the use of the Wigner–Eckart theorem these terms are finally recast into the $F$ $M_F$-parity basis. We will not explicitly express terms here but refer to, e.g., Ref. [9].

The Stark effect for a single NO molecule in its first-excited electronic state, $J=3/2$ is demonstrated in Fig. 1. In the absence of a magnetic field, the hyperfine components are degenerate for $|M_F|$ levels. The opposite-parity states repel as the field is increased. In the large-$\mathcal{E}$ limit parity ceases to be a good quantum number. In this case we follow convention and label the lower and upper states of the doublet as $e$ and $f$ states, respectively (see below). The critical field where the Stark effect transforms from quadratic to linear is around $\mathcal{E}_0=\Delta_\Lambda/2d\sim 7$ V/cm, based on the dipole moment of NO, $d=0.15872$ D [15]. For fields larger than $\mathcal{E}_0$ the $H_S$ term dominates over the hyperfine $H_{HFS}$ term in the molecular effective Hamiltonian and $F$ is no longer a good quantum number. However, $H_S$ commutes with $F_Z$, resulting in a block-diagonal Hamiltonian matrix elements with respect to the magnetic quantum number $M_F$.

To transform smoothly from the zero-field $\Lambda$-doubling Hamiltonian basis to the strong field basis for fixed values of $J$ and $M$, it is convenient to introduce a mixing angle $\delta_M$ and denote lower and upper states of $\Lambda$-doublet pairs by

$$|e\rangle=\cos\delta_M\left|^2\Pi_{3/2}^+\right\rangle-\sin\delta_M\left|^2\Pi_{3/2}^-\right\rangle, \quad (3)$$

$$|f\rangle=\sin\delta_M\left|^2\Pi_{3/2}^+\right\rangle+\cos\delta_M\left|^2\Pi_{3/2}^-\right\rangle. \quad (4)$$

The Stark Hamiltonian in the $\{|e\rangle,|f\rangle\}$ basis can be represented by

$$H_S=-\frac{d\mathcal{E}M|\Omega|}{J(J+1)}\begin{bmatrix}\cos 2\delta_M & \sin 2\delta_M\\ \sin 2\delta_M & -\cos 2\delta_M\end{bmatrix}.$$

In the limiting cases $\delta_M=0$, which corresponds to a very high field, the Stark Hamiltonian matrix is a diagonal matrix in the basis $\{|e\rangle=|^2\Pi_{3/2}^+\rangle,|f\rangle=|^2\Pi_{3/2}^-\rangle\}$, and for $\delta_M=\pi/4$ that corresponds to the zero-field limit the Stark Hamiltonian is off-diagonal in the basis $\{|e\rangle=(|^2\Pi_{3/2}^+\rangle-|^2\Pi_{3/2}^-\rangle)/\sqrt{2},|f\rangle=(|^2\Pi_{3/2}^+\rangle+|^2\Pi_{3/2}^-\rangle)/\sqrt{2}\}$. By contrast, the $\Lambda$-doubling Hamiltonian

$$H_\Lambda=\Delta_\Lambda/2\begin{bmatrix}-\sin 2\delta_M & \cos 2\delta_M\\ \cos 2\delta_M & \sin 2\delta_M\end{bmatrix}$$

is diagonal in the low-field limit $\delta_M=\pi/4$.

In an applied homogenous magnetic field the molecular magnetic moment interacts with the field and consequently the energy levels are subjected to the Zeeman effect with the Zeeman interaction Hamiltonian operator $H_Z=-\vec{\mu}_s\cdot\vec{B}$, where $\vec{\mu}_s$ is the magnetic moment in the space-fixed reference frame. Unlike the $|\Omega|=1/2$ state for which the orbital and spin contribution to the molecular magnetic moment nearly cancel, the magnetic moment of the $|\Omega|=3/2$ state ($J=3/2$) is large. The Landé factor $g_J=(g_L\Lambda+g_S\Sigma)\Omega/[J(J+1)]=0.777246$ [16], where $g_L$ and $g_S$ are electron orbital and spin $g$ factors, respectively. The Zeeman splitting is shown in Fig. 2 for the field range 0–200 G at which the stretched molecular states are split by an energy shift comparable to the Stark shift at the range of 0–6000 V/cm. We focus on the low-field seeking state of highest energy which is the stretched state with quantum numbers $|5/2,5/2;f\rangle$ for collisions.

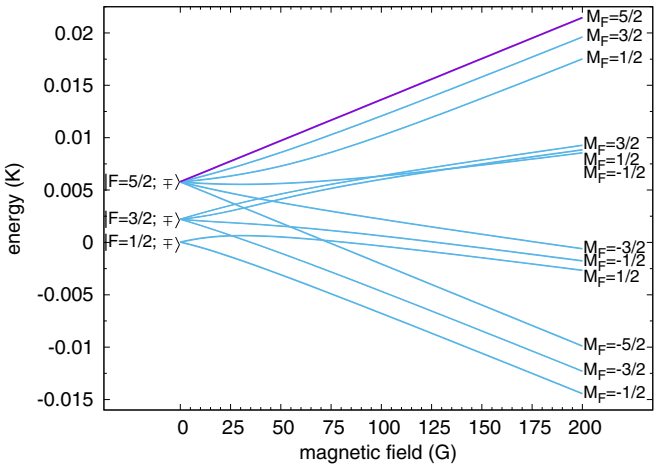


FIG. 2. Zeeman energies of the hyperfine $|F,M_F;e/f\rangle$ and $\Lambda$-doublet levels for $J=3/2$ of the $^2\Pi_{3/2}$ state of the NO molecule at zero electric field. In a detailed resolution each line would be $p$-doubly split. The hyperfine state of interest, $|5/2,5/2;f\rangle$, is highlighted.

The electric- and magnetic-field configuration can be arbitrary with an angle $\theta_{\mathcal{E}B}$ between them. In the following we set $\theta_{\mathcal{E}B} = 0$ because the electric dipoles are more easily induced when electric and magnetic moments are parallel [10] and also because $M_F$ is a conserved quantum number.

Figures 1 and 2 appear remarkably similar on the scale shown, showing the range over which the two fields produce comparable energy shifts. However, the states belonging to these spectra are quite different. Consider the stretched state $|5/2,5/2;f\rangle$ of interest. This state is doubly degenerate between states with $M_F = \pm 5/2$ and the same $f$. The states immediately lower in energy, in large electric field, differ by changing $M_F$, but still retain the $f$ parity. By contrast, the stretched state at high field in Fig. 2 is nearly degenerate in $e$ or $f$ parity, but has a unique, positive value of $M_F = +5/2$. The state immediately lower in energy changed $M_F$, but still has both parity states $e$ and $f$. These differences will matter below, in determining the dominant inelastic-scattering channels.

### C. NO-NO interaction Hamiltonian

Let us now consider scattering due to the collision of two NO molecules of mass $m$, and located at $\vec{r}_1, \vec{r}_2$, respectively. We restrict our discussion to two-body scattering in the center-of-mass frame by considering the relative position $\vec{R} = \vec{r}_1 - \vec{r}_2$ of body 1 with respect to body 2, and reduced mass $m_{\rm red} = m/2$ associated with the relative motion. In spherical coordinates we are able to solve the scattering problem by using a separation of angular and radial variables of the total wave function $\Psi(R,\theta,\phi)$; the system is subjected to the centrifugal potential $\hbar^2 L(L+1)/(2m_{\rm red}R^2)$.

For a pair of $^{14}N^{16}O$ fermionic molecules the wave function is antisymmetric with respect to interchange of the molecules. The effect of the inversion of the coordinates of all particles in the molecular center of mass is given by $E^*(R,\theta,\phi) = (R,\pi - \theta,\phi+\pi)$, thus the exchange properties of the partial waves are governed strictly by the properties of the spherical harmonics. Spherical harmonics have a definite parity $(-1)^L$ with respect to inversion about the origin, which means that the spatial wave function is inversion-antisymmetric for odd $L$ and vice versa.

Considering collisions of identical species we must use the symmetrized combinations of the uncoupled hyperfine representation $|F_1,M_{F1};p_1\rangle|F_2,M_{F2};p_2\rangle|L,M_L\rangle$. The symmetrized functions (for $F_1 \neq F_2$ or $M_{F1} \neq M_{F1}$ or $p_1 \neq p_2$) are

$$\begin{aligned}&|F_1,M_{F1};p_1\rangle|F_2,M_{F2};p_2\rangle|L,M_L\rangle_S\\ &\quad= \frac{1}{\sqrt{2}}\{|F_1,M_{F1};p_1\rangle|F_2,M_{F2};p_2\rangle|L,M_L\rangle\\ &\qquad\pm(-1)^L|F_2,M_{F2};p_2\rangle|F_1,M_{F1};p_1\rangle|L,M_L\rangle\},\end{aligned} \tag{5}$$

with the $+$ sign for bosonic molecules and the $-$ sign for fermionic molecules. In the case of indistinguishable fermionic NO molecules this relation immediately ensures that only odd partial waves are allowed in a totally antisymmetric wave function.

The potential-energy surface between the molecules includes a van der Waals interaction and is represented as $-C_6/R^6$, which we assume is isotropic in the present calculation. We take $C_6 = 35.2E_h a_0^6$ as a lower estimate of actual $C_6$ obtained from the London formula and the mean dipole static polarizability for the NO molecule [17]. We are interested in the effects of long-range forces, and in particular dipole-dipole interactions, which are dominant at long range in ultracold scattering. For this reason we simply replace the short-range physics with a hard-wall boundary condition at $R = 30a_0$. On this distance scale, the higher-excited rotational states are unlikely to be relevant.

The long-range interaction is dominated by electric dipole-dipole interaction between the two molecules:

$$\begin{aligned}V_{\rm dd}(\vec{R}) &= -\frac{3(\hat{R}\cdot\vec{d}_1)(\hat{R}\cdot\vec{d}_2) - \vec{d}_1\cdot\vec{d}_2}{4\pi\varepsilon_0 R^3}\\ &= -\frac{\sqrt{30}d^2}{4\pi\varepsilon_0 R^3}\sum_{q;q_1,q_2}(-1)^q C^2_q \begin{pmatrix}2 & 1 & 1\\ q & -q_1 & -q_2\end{pmatrix} C^1_{q_1} C^1_{q_2},\end{aligned} \tag{6}$$

where $\vec{R} = R\hat{R}$ is the intermolecular separation vector in relative coordinates, and $\vec{d}_i$ is the electric dipole of molecule $i$. $C^1_{q_i}$ and $C^2_q$ are components of first- and second-rank spherical tensors, which are given by reduced spherical harmonics. The term $V_{\rm dd}$ can be given in a matrix representation in the symmetrized hyperfine basis (5), as written, e.g., in Ref. [18] with a remaining dependence on the radial coordinate $R$.

The space-fixed reference frame collisional Hamiltonian for the NO-NO molecular system whose point mass is located at the center of mass is

$$H_{\rm tot} = -\frac{\hbar^2}{2m_{\rm red}}\frac{d^2}{dR^2} + H_{1,2} + V, \tag{7}$$

where $H_{1,2} = H_1 \otimes \mathbb{1}_2 + \mathbb{1}_1 \otimes H_2$ is the sum of the one-molecule effective Hamiltonians, $V$ is the general term of potential energy including centrifugal barrier, long-range isotropic van der Waals interactions, and anisotropic dipole-dipole interactions.

The total wave function $\Psi(\vec{R})$ is represented by a column vector having the $n$th component of the form

$$\Psi_n(\vec{R}) = \frac{\psi_n(R)}{R}[|F_1,M_{F1};p_1\rangle|F_2,M_{F2};p_2\rangle|L,M_L\rangle_S],$$

where $n$ is a collective index denoting all the channel indices in the square brackets, and $\psi_n$ is the diabatic solution of the set of coupled radial equations

$$\left[\sum_{m=1}^{N_{\rm ch}}\left(-\frac{\hbar^2}{2m_{\rm red}}\frac{d^2}{dR^2} + E_m\right)\delta_{nm} + V_{nm}\right]\psi_m = E_{\rm tot}\psi_n, \tag{8}$$

with $E_m$ being the threshold energy of channel $m$, which is defined as the eigenenergy of $H_{1,2}$ in the $R\to\infty$ limit. $E_{\rm tot}$ represents the total collision energy, which is a conserved quantity during the collision. The total energy $E_{\rm tot} = E_{\rm c} + E_n$, where $E_{\rm c}$ is the collision energy relative to the threshold energy $E_n$ of the incident channel.

In addition to symmetric properties of the wave functions another molecular symmetry of great importance for the interaction Hamiltonian is the total molecular angular-momentum projection onto an electric-field axis, $M_{\rm tot} = M_{F1} + M_{F2} + M_L$. This quantum number is conserved in an electric field by dipole-dipole interactions and the same holds for magnetic fields.

The set of coupled Schrödinger equations (8) in multichannel scattering was solved by employing the log-derivative propagator method [19]. Matching the log-derivative matrix with the asymptotic solution for open channels at large $R$ yields the open-open submatrix of the reaction $K$ matrix, and subsequently the scattering matrices $S$ and $T$. The partial scattering cross section for a collision process between an inbound channel $i$ and any of the outbound channels $f$ is given by

$$\sigma_{L,i\to f}(E) = 2 \times \frac{\pi}{k_i^2} \sum_{M_L} \sum_{f,L',M_L'} |\langle i,L,M_L|T|f,L',M_L'\rangle|^2,$$

where $f = i$ for elastic processes and $f \neq i$ for inelastic processes, $k_i^2 = 2m_{\rm red}(E_{\rm tot} - E_i^{1,2})/\hbar^2 = 2m_{\rm red}E_{\rm c}/\hbar^2$ a square of the wave number of an incident channel, and the numerical factor of two is required because of permutation symmetry in collisions of identical particles in indistinguishable hyperfine states. The total cross section is a sum of partial cross sections over all possible incoming partial waves $L$

$$\sigma_{i\to f}(E) = \sum_L \sigma_{L,i\to f}(E).$$

We also consider scattering rate constants, defined as $K = v_i\sigma$, where $v_i$ is the incident collision velocity.

In practice, we consider only scattering within the $|\Omega| = 3/2$ manifold and disregard possible collision events where molecules scatter into $|\Omega| = 1/2$ states, which are far away in energy. Within this approximation, and for the $|5/2,5/2;f\rangle|5/2,5/2;f\rangle$ initial state of interest, we find that including partial waves $L = 1, 3, 5$ is sufficient to converge the cross sections to perhaps 20 percent at the highest energies considered, a sufficient convergence for our computation purposes. At the lowest collision energy of $10^{-5}$ K a right bound of $15\,000a_0$ is sufficient to have a converged cross section below 5%. Within these approximations there are $N_{\rm ch} = 258$ total scattering channels.

## III. SCATTERING RESULTS

We have calculated the elastic and inelastic cross sections for colliding molecules subjected to magnetic and electric fields. Note that, by elastic is meant collisions during which the internal state $|F,M_F;p\rangle$ of both molecules remains unchanged, whereas by inelastic is meant collisions in which at least one molecule converts its internal state to another. The collision energy within the wide range of 10 $\mu$K through 1 K is considered. As a rule of thumb, we seek circumstances where the ratio of elastic to inelastic collision rates is 100 or greater, to facilitate evaporative cooling.

Figure 3 shows cross sections for $\mathcal{E} = 6000$ V/cm and $B = 1000$ G with partial-wave contributions to the total cross sections. Below 1.5 mK the inelastic collisions dominate over the elastic collisions. At around $10^{-4}$ K the inelastic cross section features a maximum. Below this energy lies the threshold regime where $\sigma_{\rm inel}$ scales with collision energy $E_{\rm c}$ as $E_{\rm c}^{1/2}$. Above this energy, $\sigma_{\rm inel} \sim E_{\rm c}^{-2}$. For the indicated values of the electric and magnetic field the favorable ratio of at least one hundred elastic events to one inelastic collision event seems to hold from 100 mK to higher collision energies, thus allowing NO molecules to be cooled by collisions to this limit.

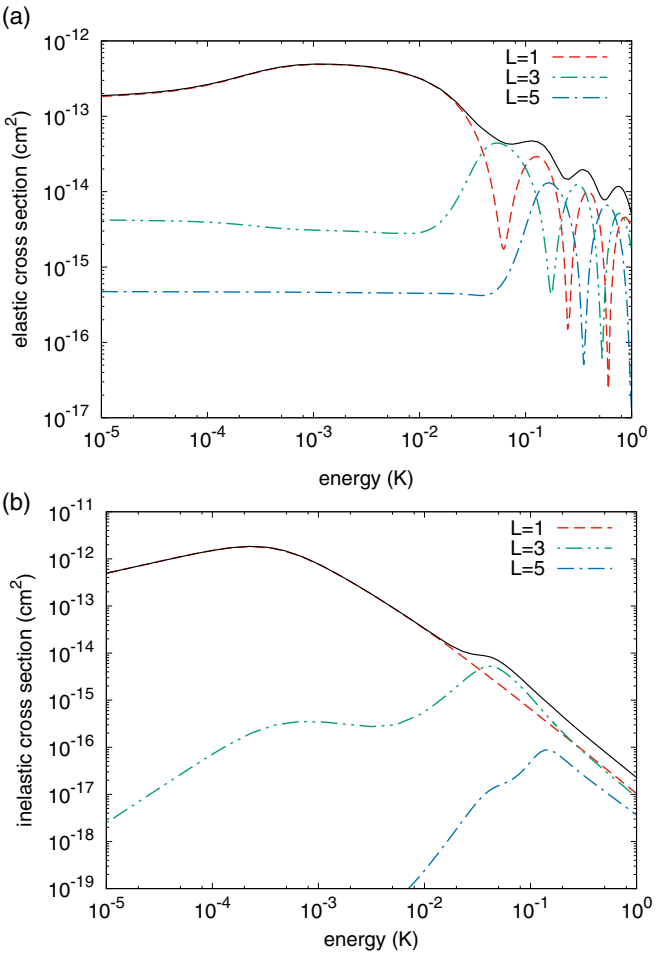


FIG. 3. (a) Elastic and (b) inelastic cross sections versus the collision energy for 6000 V/cm applied electric field and 1000 G applied magnetic field. Also shown are the individual partial-wave contributions $L = 1, 3, 5$ to the total cross section calculated in the inbound channel $|5/2,5/2;f\rangle|5/2,5/2;f\rangle|1,0\rangle_S$.

Figure 3 closely resembles the similar Fig. 3 in Ref. [1], which showed the result for the $|\Omega| = 1/2$ state of the NO molecule, also in an electric field $\mathcal{E} = 6000$ V/cm. It differs, of course, in that the $|\Omega| = 1/2$ had no magnetic moment and would not have been influenced by a magnetic field. The fact that the overall magnitude and variation of the cross sections is similar between the $|\Omega| = 3/2$ and $|\Omega| = 1/2$ states, is reasonable since the principal physics being explored here is due to the electric-dipole interactions between the molecules. There are also differences in the two cases, which likely arise from details of angular-momentum coupling in the $|\Omega| = 3/2$ versus $|\Omega| = 1/2$ state, and particularly in the hyperfine structure.

The effect of the magnetic field on the $|\Omega| = 3/2$ state can be significant. To see this, we examine scattering-rate coefficients in zero electric field, as shown in Fig. 4, for collision energies $E_{\rm c} = 100$ mK and $E_{\rm c} = 1$ mK. Figure 4 plots rate coefficients versus magnetic-field strength. At the low collision energy of 1 mK, the inelastic rate actually exceeds the elastic rate, until a field of about 2000 G is applied. At still higher fields, the inelastic rate continues to diminish. Nevertheless, the ratio of

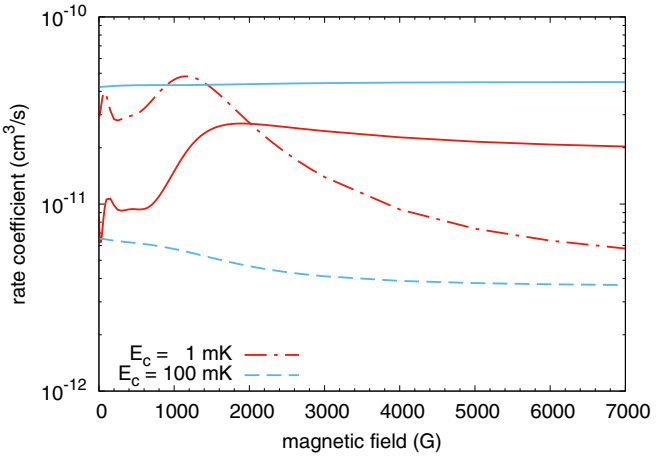


FIG. 4. Rate coefficient for elastic (solid curves) and inelastic (dashed curves) as a function of magnetic field at $E = 0$ V/cm for the two different collision energies: $E_c = 1$ mK (red, dark curve) and $E_c = 100$ mK (blue, light curve).

elastic to inelastic scattering remains less than an order of magnitude for the fields considered. Qualitatively, the same behavior is seen for $E_c = 100$ mK, although elastic scattering already exceeds inelastic scattering in zero field. The general conclusion, from the point of view of evaporative cooling, is that a magnetic field does not sufficiently increase the ratio of elastic to inelastic scattering.

The presence of a magnetic field can also strongly influence the behavior of rate constants when an electric field is present. This influence is indicated in Fig. 5. Panel (a) of this figure shows rate coefficients versus electric field for a low collision energy, $E_c = 1$ mK. In the absence of a magnetic field (black lines), the inelastic rate actually far exceeds the elastic rate for most of the range; a situation similar to the case in the $|\Omega| = 1/2$ state (see Fig. 4 of Ref. [1]). Incorporating a magnetic field parallel to the electric field can ameliorate this difference: elastic and inelastic rates are comparable for all electric fields if the magnetic field is 1000 G (red lines); while the elastic rate exceeds the inelastic rate for all electric fields if $B = 3000$ G (blue lines). Moreover, large electric fields tend to suppress the inelastic rates while leaving the elastic rates alone, an effect already emphasized for the $|\Omega| = 1/2$ state. Admittedly, the fields required for this suppression are unrealistically large to be a useful means of achieving evaporative cooling at millikelvin temperatures.

The situation is somewhat more promising in the case of 100 mK collision energy [Fig. 5(b), zoom to small electric field in Fig. 5(c)]. Here inelastic scattering is already suppressed in zero field and becomes further suppressed as the magnetic field is increased. Meanwhile, the elastic-scattering rate is essentially unchanged by the magnetic fields. In a $B = 3000$ G magnetic field, it is conceivable that merely polarizing the atoms ($\mathcal{E} > 40$ V/cm) is sufficient to promote evaporative cooling to this temperature.

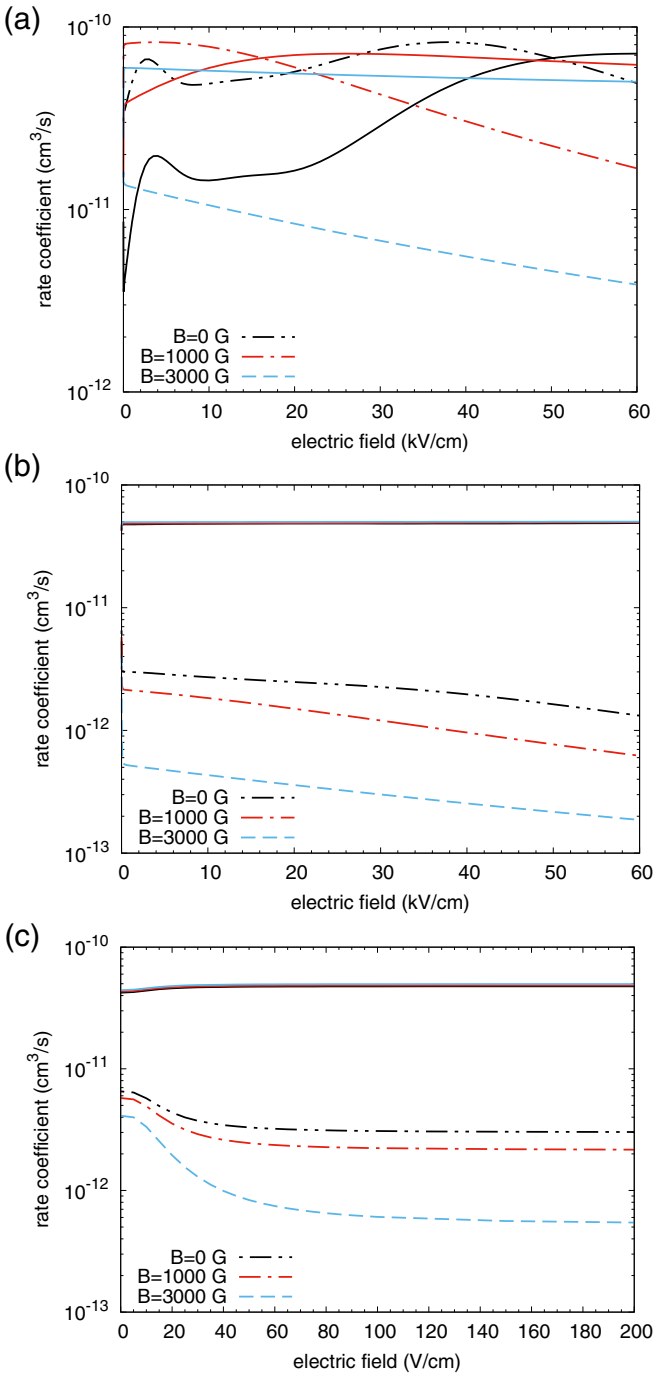


FIG. 5. Rate coefficients for elastic (solid curves) and inelastic (dashed curves) scattering as a function of electric field at $B = 0$ G (black curve), $B = 1000$ G (red curve), and $B = 3000$ G (light blue curve). The collision energy is fixed at the value (a) $E_c = 1$ mK, (b) $E_c = 100$ mK. (c) The same as in panel (b) but in detailed electric-field range.

## IV. SEMI-QUANTITATIVE ANALYSIS

Regardless of some inelastic suppression at large fields and at temperatures above 10 mK, inelastic scattering is nevertheless a fact of life for these radicals. It is worthwhile to look at the mechanism of inelastic scattering, both to see why this scattering occurs, and why it is suppressed.

Starting from the stretched state $|5/2,5/2; f\rangle|5/2,5/2; f\rangle$, collisions can be inelastic, thereby releasing energy, by transformations of two types: either the molecules can change

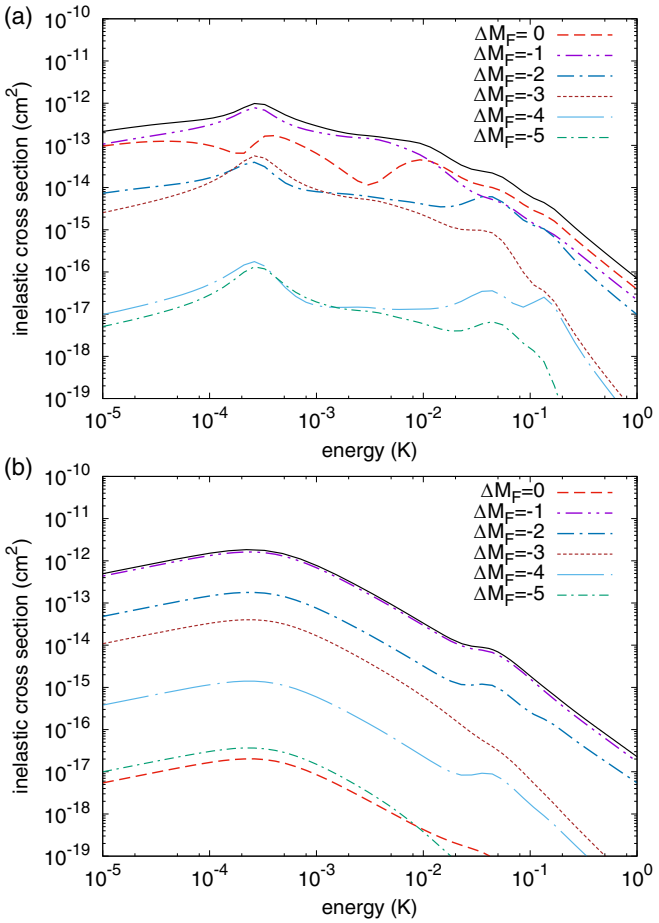


FIG. 6. Inelastic cross sections versus collision energy (a) in the absence of field, (b) subjected to an electric field of $\mathcal{E} = 6000$ V/cm and a magnetic field of $B = 1000$ G. The collisions occur in the incident state $|5/2, M_{F1} = 5/2; f\rangle|5/2, M_{F2} = 5/2; f\rangle|1,0\rangle_S$ and individual partial cross sections represent losses to channels that change $M_{F1}$ and $M_{F2}$. The notation $\Delta M_F = M'_{F1} - M_{F1} + M'_{F2} - M_{F2}$.

the total projection of angular momentum on the field axis, $\Delta M_F = \Delta M_{F1} + \Delta M_{F2}$, with the shed angular momentum transferred to partial-wave angular momentum; or else one or both molecules can change parity state from $f$ to $e$.

The partial cross sections for the various $\Delta M_F$ channels are shown in Fig. 6, both in the absence of applied field [Fig. 6(a)] and in fields of $\mathcal{E} = 6000$ V/cm and $B = 1000$ G [Fig. 6(b)]. Quite generally, these partial cross sections exhibit a propensity rule, whereby larger changes in angular momentum, $\Delta M_F$, are suppressed relative to smaller changes. A notable exception is the partial cross section for $\Delta M_F = 0$. In zero field this process is somewhat suppressed with respect to $\Delta M_F = -1$ for energies below $\sim$10 mK, while in strong fields it is suppressed to be the least significant cross section of all.

The ability of the molecules to scatter into different $\Delta M_F$ and parity channels depends qualitatively on two things: the initial-to-final-state coupling, and the energy released in the collision. This can be seen in the plane-wave Born approximation, where the transition amplitude between initial channel $i$ with wave number $k_i$ and parities $p_{1i}$, $p_{2i}$, to final channel $f$ with wave number $k_f$ and parities $p_{1f}$, $p_{2f}$, is given by [7]

$$\langle i|T|f\rangle = \frac{4m_{\rm red}}{\hbar^2} C_{i,f}\sqrt{k_i k_f}\int_0^\infty \frac{j_{L_i}(k_i R) j_{L_f}(k_f R)}{R} dR$$
$$= A C_{i,f}\sqrt{k_i k_f}\frac{k_i^{L_i}}{k_f^{L_f}} F(a,b,c;(k_i/k_f)^2). \quad (9)$$

Here $k_i$ and $k_f$ are the wave numbers of the initial and final channels; $F$ is a hypergeometric function whose indices depend on angular-momentum quantum numbers; and $C_{if}$ are matrix elements of the dipole coupling in the dressed states of the molecules, exclusive of the $1/R^3$ scaling.

The matrix elements $C_{if}$ depend strongly on electric field, which can be seen as follows: In the expression (6) for the dipolar interactions, the matrix elements of the individual $C^1_{q_i}$ components is given by

$$C^1_{q_i} = \langle J, M, |\Omega| | C^1_{q_i} | J, M, |\Omega|\rangle \begin{bmatrix} \cos 2\delta_M & \sin 2\delta_M \\ \sin 2\delta_M & \cos 2\delta_M \end{bmatrix},$$

using [20]

$$\langle J, M, \Omega | C^1_{q_i} | J, M, \Omega'\rangle = \frac{\delta_{\Omega,\Omega'}\Omega}{J(J+1)} \begin{cases} M, & q_i = 0 \\ \pm\sqrt{\frac{J^2 - M^2}{2}}, & q_i = \mp 1. \end{cases}$$

Thus in the two-molecule field-dressed basis the $C_{i,f}$ matrix elements depend on the parity states and the electric field (via $\delta_M$) as

$$\langle ee|C|ee\rangle \propto \cos^2(2\delta_M),$$
$$\langle ee|C|ef\rangle \propto \sin(4\delta_M), \quad (10)$$
$$\langle ee|C|ff\rangle \propto \sin^2(2\delta_M),$$

Thus in the zero-electric-field limit, $\delta_M \to \pi/4$, the initial channel with $p_{1i} = p_{2i} = f$ is directly coupled only to the final channel with $p_{1f} = p_{2f} = e$; both molecules must change parity. Whereas in the high-electric-field limit, $\delta_M \to 0$ and the initial channel $p_{1i} = p_{2i} = f$ couples only to channels where $p_{1f} = p_{2f} = f$ also; that is, the $f$ character of the state is preserved.

The second effect, that of the energy released in the collision, follows from the Born-approximation result, noting that in the threshold limit $k_i/k_f \to 0$, the hypergeometric function in Eq. (9) is reduced to unity. The energy dependence is therefore in the prefactor $\sqrt{k_i k_f} k_i^{L_i}/k_f^{L_f}$. For final wave numbers given by the energy released, $k_f = (2m_{\rm red}\Delta E/\hbar^2)^{1/2}$, where $\Delta E$ is the energy between incident and final thresholds, and for $p$ waves $L_f = 1$, we have $\sigma_{if} \propto 1/\sqrt{\Delta E}$, which is suppressed as the gap $\Delta E$ gets larger. This idea was used to explain the electric-field suppression of inelastic rates in Ref. [1].

Selected rate constants in the Born approximation, with $\Delta M_F = -1, 0$, are shown in Fig. 7. The rates show the smooth transition between $ee$ final states that are the dominant result at zero field, to the $ff$ final states that dominate at large field. At small electric field, both $\Delta M_F = -1, 0$ channels with opposite $ee$ parity are readily available, with gap $\Delta E$ remaining small, on the order of the $\Lambda$-doubling energy. Both possibilities are therefore approximately equally likely.

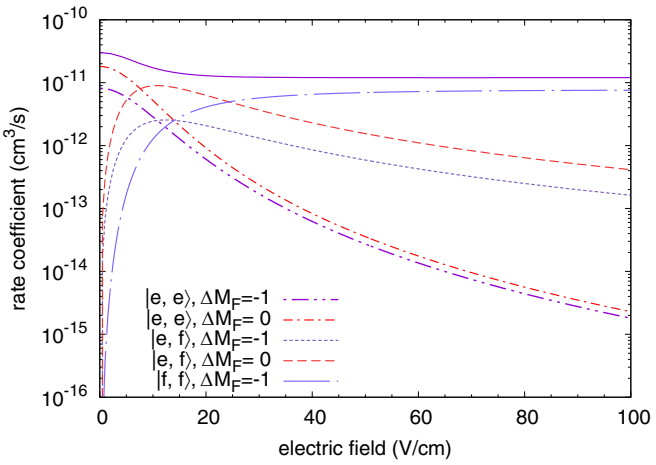


FIG. 7. Rate coefficients in Born approximation for inelastic scattering as a function of electric field at $B = 0$ G between the incident channel $|f,f\rangle \equiv |5/2,M_{F1} = 5/2;f\rangle|5/2,M_{F2} = 5/2;f\rangle|1,0\rangle_S$ and final channels indicated in the legend that are either of different $e$ (or $f$) parity or different $M_F$. The collision energy is fixed at the value $E_c = 1$ mK. The solid purple curve corresponds to a sum of all $\Delta M_F = -1$ state-changing collisions, where only selected dominant $K_{i\to f}$ are shown. Only the $L_f = 1$ outcoming partial wave is considered.

On the other hand, at large field, a parity-conserving $\Delta M_F = -1$ transition, $|5/2,5/2;f\rangle|5/2,5/2;f\rangle \to |5/2,5/2;f\rangle|5/2,3/2;f\rangle$ is easily allowed, with a gap corresponding to approximately the hyperfine splitting (Fig. 1), so this transition proceeds rapidly. But for a $\Delta M_F = 0$ transition, the only parity-preserving operation is $|5/2,5/2;f\rangle|5/2,5/2;f\rangle \to |5/2,5/2;f\rangle|5/2,5/2;f\rangle$; that is, elastic scattering. The $\Delta M_F = 0$ inelastic transition is therefore highly suppressed.

Finally, we note that, for any allowed transition, such as the $\Delta M_F = -1$ transition, $|5/2,5/2;f\rangle|5/2,5/2;f\rangle \to |5/2,5/2;f\rangle|5/2,3/2;f\rangle$ at high field, the addition of a magnetic field further splits the energy between the $|5/2,5/2\rangle$ and $|5/2,3/2\rangle$ states, increasing the gap $\Delta E$ and further somewhat suppressing the inelastic rates. This is the result seen in Fig. 5.

## V. CONCLUSIONS

We analyzed the possibility of evaporative cooling of NO molecules in their $|\Omega| = 3/2$, $J = 3/2$ state and computed scattering cross sections and rate coefficients under the influence of electric and magnetic fields. We find that evaporative cooling is viable only for collision energies $E_c$ no lower than $\sim$100 mK, which is similar to a result obtained for NO in the $^2\Pi_{1/2}$ state [1]. Without the influence of an external magnetic field, the ratio of elastic to inelastic rates is highly unfavorable and does not exceed 100 at $E_c = 100$ mK even when an unrealistically high electric field is applied. Magnetic fields of a few thousand gauss are necessary for effective cooling, the suppression of the inelastic rate can then be controlled by an additional electric field, which is in accordance with the phenomenon found for the $^2\Pi_{1/2}$ state [1].

As a result, no matter what field is applied and of what magnitude, the most probable inelastic process is the one that changes the sum of total-angular-momentum projection $\Delta M_F$ for both collision species by one.

Finally, we discussed the role of molecular state parity that is during inelastic processes preferred to be changed or conserved with respect to the magnitude of the electric field.

## ACKNOWLEDGMENTS

We acknowledge funding from the U.S. Army Research Office under ARO Grant No. W911NF-12-1-0476 and from the JILA NSF Physics Frontier Center, PHY-1734006. L.D.A. acknowledges the financial support of the Czech Science Foundation (Grant No. P209/18-00918S).

[1] L. D. Augustovičová and J. L. Bohn, Phys. Rev. A **96**, 042712 (2017).
[2] S. N. Vogels, J. Onvlee, S. Chefdeville, A. van der Avoird, G. C. Groenenboom, and S. Y. T. van de Meerakker, Science **350**, 787 (2015).
[3] Z. Gao, S. N. Vogels, M. Besemer, T. Karman, G. C. Groenenboom, A. van der Avoird, and S. Y. T. van de Meerakker, J. Phys. Chem. A **121**, 7446 (2017).
[4] X. Wang, M. Kirste, G. Meijer, and S. Y. T. van de Meerakker, Z. Phys. Chem. **227**, 1595 (2013).
[5] K. E. Strecker and D. W. Chandler, Phys. Rev. A **78**, 063406 (2008).
[6] L. M. C. Janssen, A. van der Avoird, and G. C. Groenenboom, Phys. Rev. Lett. **110**, 063201 (2013).
[7] A. V. Avdeenkov and J. L. Bohn, Phys. Rev. A **71**, 022706 (2005).
[8] J. L. Bohn, A. M. Rey, and J. Ye, Science **357**, 1002 (2017).
[9] C. Ticknor and J. L. Bohn, Phys. Rev. A **71**, 022709 (2005).
[10] G. Quéméner and J. L. Bohn, Phys. Rev. A **88**, 012706 (2013).
[11] B. K. Stuhl, M. T. Hummon, M. Yeo, G. Quéméner, J. L. Bohn, and J. Ye, Nature (London) **492**, 396 (2012).
[12] D. Reens, H. Wu, T. Langen, and J. Ye, Phys. Rev. A **96**, 063420 (2017).
[13] T. D. Varberg, F. Stroh, and K. M. Evenson, J. Mol. Spectrosc. **196**, 5 (1999).
[14] W. Meerts and A. Dymanus, J. Mol. Spectrosc. **44**, 320 (1972).
[15] D. R. Lide, *CRC Handbook of Chemistry and Physics*, 84th ed. (CRC Press, Boca Raton, FL, 2003).
[16] R. L. Brown and H. E. Radford, Phys. Rev. **147**, 6 (1966).
[17] N. J. Bridge and A. D. Buckingham, Proc. R. Soc. London, Ser. A **295**, 334 (1966).
[18] A. V. Avdeenkov and J. L. Bohn, Phys. Rev. A **66**, 052718 (2002).
[19] B. R. Johnson, J. Comput. Phys. **13**, 445 (1973).
[20] J. L. Bohn, in *Cold Molecules: Theory Experiment, Applications*, edited by R. V. Krems, B. Friedrich, and W. C. Stwalley (CRC Press, Taylor & Francis Group, Boca Raton, FL, 2010), Chap. 2, p. 39.